Finite-temperature quantum condensations in the space of states: A different perspective on quantum annealing

Massimo Ostilli [1] and Carlo Presilla [2,3]

[1]*Instituto de Física, Universidade Federal da Bahia, Salvador, 40210-340, Bahia, Brazil*
[2]*Dipartimento di Matematica, Sapienza Università di Roma, Piazzale A. Moro 2, 00185 Rome, Italy*
[3]*Istituto Nazionale di Fisica Nucleare, Sezione di Roma 1, 00185 Rome, Italy*

In nature, everything occurs at finite temperature, and quantum phase transitions (QPTs) cannot be an exception. Nevertheless, they are still mainly discussed and formulated at zero temperature. We show that the condensation QPTs recently introduced at zero temperature can naturally be extended to finite temperature just by replacing ground-state energies with corresponding free energies. We illustrate this criterion in the paradigmatic Grover model and in a system of free fermions in a one-dimensional inhomogeneous lattice. In agreement with expected universal features, the two systems show structurally similar phase diagrams. Last, we explain how finite-temperature condensation QPTs can be used to construct quantum annealers having, at finite temperature, output probability exponentially close to 1 in the system size. As examples we consider again the Grover model and the fermionic system, the latter being well within the reach of present heterostructure technology.

I. INTRODUCTION

Quantum phase transitions (QPTs), i.e., the thermodynamic singularities emerging at zero temperature ($T = 0$) driven by some Hamiltonian parameter of the system, originate from quantum fluctuations, a consequence of Heisenberg's uncertainty principle. However, an isolated system at $T = 0$ represents an abstract limit, and understanding the finite-temperature counterpart of a QPT (if any) is of paramount importance. Such an aim represents a quite challenging issue, from both theoretical and experimental viewpoints, since, above zero temperature, quantum and thermal fluctuations may compete in an intricate manner.

Put in simple terms, in general, two kinds of scenarios are expected [1–8]: the ordered phase exists only at zero temperature; the ordered phase exists also at finite temperature below some critical value T_c which, in turn, might signal a purely classical phase transition when the Hamiltonian parameters are set to a value rendering the system classical (e.g., the Ising model in a transverse field becomes the classical Ising model when the transverse field is set to zero).

This second scenario is particularly appealing for potential applications to quantum annealing protocols aimed at finding the ground state (GS) by working at finite temperature, the GS of the ordered phase being the solution of some (classical) combinatorial problem of interest, possibly hard [9–11]. First-order QPTs, a much less explored field when compared to second-order QPTs, might favor this scenario since, at the transition, the order parameter jumps between two very different quantum states, possibly orthogonal.

For concreteness, let us consider systems described by a Hamiltonian of the form

$$H = \Gamma K + JV, \qquad (1)$$

where K and V are two noncommuting dimensionless Hermitian operators and Γ and J are parameters with energy dimensions. Representing H in the eigenbasis of V, it is natural to call V the potential operator, K the hopping operator, Γ the hopping parameter, and J the potential strength. We will use, equivalently, Γ or J as the control parameter of the supposed QPT. Since phase transitions occur in the thermodynamic limit (TDL), we need a fair competition between K and V in this limit. By this we mean that, supposing that H describes a system of N particles or spins, the eigenvalues of K and V both scale linearly with N.

Recently, we introduced a class of first-order QPTs taking place, at $T = 0$, via a condensation in the space of states [12]. Consider a partition of the space of states $\mathcal{H}$ of the system into two subspaces, $\mathcal{H} = \mathcal{H}_{\mathrm{cond}} \oplus \mathcal{H}_{\mathrm{norm}}$, such that, in the TDL, $\dim \mathcal{H}_{\mathrm{cond}} / \dim \mathcal{H} \to 0$, and suppose to follow, for a very large time t, the evolution of an initial quantum state belonging to $\mathcal{H}_{\mathrm{cond}}$. A heuristic, ergodicity-breaking argument applies which is inspired by the exact probabilistic representation of the quantum evolution introduced in [13]: due to the fact that $\mathcal{H}_{\mathrm{cond}}$ has vanishing relative dimension, in the TDL, the system will spend a vanishing fraction of t inside $\mathcal{H}_{\mathrm{cond}}$ *unless* it finds that it is energetically more convenient to remain in $\mathcal{H}_{\mathrm{cond}}$. In other words, at $T = 0$, in the TDL the energy of the system becomes the minimum between the GS energies of H restricted to $\mathcal{H}_{\mathrm{cond}}$ and $\mathcal{H}_{\mathrm{norm}}$. Now, if for some finite value of the Hamiltonian parameter Γ (or J), the above two GS energies cross each other, the system undergoes a first-order QPT driven by this parameter. More precisely, crossing this point, the GS of the system steeply changes from being a superposition in the *normal* subspace $\mathcal{H}_{\mathrm{norm}}$, asymptotically as large as $\mathcal{H}$, to being a superposition in the *condensed* subspace $\mathcal{H}_{\mathrm{cond}}$, with vanishing relative dimension. This is what we call a condensation QPT. Notice

that, by construction, the *normal* and *condensed* GSs are orthogonal.

In the present paper, we propose a simple criterion to extend the $T = 0$ condensation QPTs to finite temperature. For systems at canonical equilibrium at temperature T, the same phase-transition mechanism described above can take place just by replacing the GS energies with the free energies. While a mathematical proof of this criterion can be provided [14], here, we illustrate it with two examples. First, we derive analytically the phase diagram of the paradigmatic Grover model. Then, we consider a physical system, experimentally implementable, consisting of free fermions in a one-dimensional (1D) inhomogeneous lattice. In the latter case we obtain, numerically, a phase diagram that is structurally similar to that of the Grover model, in agreement with the universal features of the condensation QPTs [14]. Guided by the above two case studies, we finally show how finite-temperature condensation QPTs can be used to build quantum annealers having, at finite temperature, output probability exponentially close to 1 in the system size.

Two comments are in order about the nature of the condensation QPTs: (i) they are intrinsically first-order, for they can be driven by using even one single Hamiltonian parameter. In contrast, as for the classical case, jumps of the order parameter can result when crossing the coexistence line of two different phases that originate from the critical point of a second-order QPT. Notice that, for such a scenario to take place at zero temperature, the Hamiltonian needs to depend on at least two independent parameters (think of the 1D Ising model in the presence of both transverse and longitudinal magnetic fields [15,16]). (ii) Condensation QPTs are far from being exotic. As we recently showed at $T = 0$, the renowned Wigner crystallization belongs to this class of QPTs [17].

II. NORMAL AND CONDENSED SUBSPACES

We start by defining a proper partition of the space of states. Consider a system with Hamiltonian (1), and let $\{|\boldsymbol{n}_k\rangle\}_{k=1}^M$ be a complete orthonormal set of eigenstates of V, called *the configurations*: $V|\boldsymbol{n}_k\rangle = V_k|\boldsymbol{n}_k\rangle$, $k = 1, \ldots, M$. We assume ordered potential values $V_1 \leqslant \cdots \leqslant V_M$. Given an integer M_{cond} with $1 \leqslant M_{\mathrm{cond}} < M$, we make a partition of the set of configurations as $\{|\boldsymbol{n}_k\rangle\}_{k=1}^M = \{|\boldsymbol{n}_k\rangle\}_{k=1}^{M_{\mathrm{cond}}} \cup \{|\boldsymbol{n}_k\rangle\}_{k=M_{\mathrm{cond}}+1}^M$. Correspondingly, the Hilbert space of the system, $\mathcal{H} = \mathrm{span}\{|\boldsymbol{n}_k\rangle\}_{k=1}^M$, equipped with the standard complex scalar product $\langle u|v\rangle$, is decomposed as the direct sum of two mutually orthogonal subspaces, denoted condensed and normal, $\mathcal{H} = \mathcal{H}_{\mathrm{cond}} \oplus \mathcal{H}_{\mathrm{norm}}$, where $\mathcal{H}_{\mathrm{cond}} = \mathrm{span}\{|\boldsymbol{n}_k\rangle\}_{k=1}^{M_{\mathrm{cond}}}$ and $\mathcal{H}_{\mathrm{norm}} = \mathrm{span}\{|\boldsymbol{n}_k\rangle\}_{k=M_{\mathrm{cond}}+1}^M = \mathcal{H}_{\mathrm{cond}}^\perp$.

III. FINITE-TEMPERATURE QUANTUM CONDENSATIONS

We suppose that the system, in contact with a heat bath, is at canonical equilibrium at temperature $T = 1/(k_B\beta)$; that is, it is in the state described by the Gibbs density-matrix operator $\rho = e^{-\beta H} / \mathrm{tr}\, e^{-\beta H}$. We define the Gibbs free energies

associated with the spaces $\mathcal{H}$, $\mathcal{H}_{\mathrm{cond}}$, and $\mathcal{H}_{\mathrm{norm}}$ as

$$e^{-\beta F} = \mathrm{tr}\, e^{-\beta H} = \sum_{|\boldsymbol{n}\rangle \in \mathcal{H}} \langle \boldsymbol{n}|e^{-\beta H}|\boldsymbol{n}\rangle,$$

$$e^{-\beta F_{\mathrm{cond}}} = \mathrm{tr}_{\mathrm{cond}}\, e^{-\beta H_{\mathrm{cond}}} = \sum_{|\boldsymbol{n}\rangle \in \mathcal{H}_{\mathrm{cond}}} \langle \boldsymbol{n}|e^{-\beta H_{\mathrm{cond}}}|\boldsymbol{n}\rangle,$$

$$e^{-\beta F_{\mathrm{norm}}} = \mathrm{tr}_{\mathrm{norm}}\, e^{-\beta H_{\mathrm{norm}}} = \sum_{|\boldsymbol{n}\rangle \in \mathcal{H}_{\mathrm{norm}}} \langle \boldsymbol{n}|e^{-\beta H_{\mathrm{norm}}}|\boldsymbol{n}\rangle,$$

where H_{cond} and H_{norm} are the restrictions of H to the condensed and normal subspaces. In the representation of the eigenstates of V, H_{cond} corresponds to a null matrix except for the block $\langle \boldsymbol{n}_k|H_{\mathrm{cond}}|\boldsymbol{n}_{k'}\rangle = \langle \boldsymbol{n}_k|H|\boldsymbol{n}_{k'}\rangle$, $k, k' = 1, \ldots, M_{\mathrm{cond}}$. Analogously, H_{norm} corresponds to a null matrix except for the block $\langle \boldsymbol{n}_k|H_{\mathrm{norm}}|\boldsymbol{n}_{k'}\rangle = \langle \boldsymbol{n}_k|H|\boldsymbol{n}_{k'}\rangle$, $k, k' = M_{\mathrm{cond}} + 1, \ldots, M$. Note that $H_{\mathrm{cond}} + H_{\mathrm{norm}} \neq H$. According to the scaling properties assumed for K and V, we have that the free energies F, F_{cond}, and F_{norm} increase linearly with N (at least in the TDL).

By replacing the energies E, E_{cond}, and E_{norm} with the corresponding free energies F, F_{cond}, and F_{norm}, in analogy with the $T = 0$ case [12], we find that, if $M_{\mathrm{cond}}/M \to 0$, then up to $o(N)$ terms,

$$F \simeq \begin{cases} F_{\mathrm{cond}}, & \text{if } F_{\mathrm{cond}} < F_{\mathrm{norm}}, \\ F_{\mathrm{norm}}, & \text{if } F_{\mathrm{norm}} < F_{\mathrm{cond}}. \end{cases} \qquad (2)$$

See Appendix A for the proof. The above criterion provides an extension of the $T = 0$ condensation QPTs to finite temperature. In fact, by varying some parameter of the Hamiltonian, e.g., Γ or J, and/or the temperature T, we obtain a QPT, necessarily of first order, whenever a crossing takes place between F_{cond} and F_{norm}.

Provided that the above criterion holds true, in the TDL the space of states splits at the quantum critical line defined by

$$\lim_{N \to \infty} \frac{F_{\mathrm{cond}}}{N} = \lim_{N \to \infty} \frac{F_{\mathrm{norm}}}{N}. \qquad (3)$$

In other words, also for finite T, in the TDL we have effectively $e^{-\beta H} \to e^{-\beta(H_{\mathrm{cond}}+H_{\mathrm{norm}})}$. This allows us to define the following order parameter which definitely classifies the condensation in the space of states as a first-order phase transition:

$$p_{\mathrm{cond}} = \sum_{|\boldsymbol{n}\rangle \in \mathcal{H}_{\mathrm{cond}}} \langle \boldsymbol{n}|\rho|\boldsymbol{n}\rangle \simeq \frac{1}{1 + e^{-\beta(F_{\mathrm{norm}}-F_{\mathrm{cond}})}}, \qquad (4)$$

where the last expression is valid up to terms exponentially small in N; see Appendix A for the proof. In the TDL the free energies diverge as N, and we have $p_{\mathrm{cond}} = 1$ in the condensed phase, where $F_{\mathrm{cond}} < F_{\mathrm{norm}}$, and $p_{\mathrm{cond}} = 0$ in the normal phase, where $F_{\mathrm{norm}} < F_{\mathrm{cond}}$. At the critical line separating the two phases we have $p_{\mathrm{cond}} = 1/2$.

Apart from the necessary condition $M_{\mathrm{cond}}/M \to 0$ in the TDL, the size M_{cond} should be properly chosen so that Eq. (3) admits a solution; see [17] for a detailed discussion at $T = 0$. In particular, M_{cond} cannot be smaller than the degeneracy of the GS of V but can be bigger, as in the second example we consider.

IV. GROVER MODEL

We illustrate the mechanism of the finite-temperature condensation in the exactly solvable Grover model, a simple, yet nontrivial, example emulating a benchmark model for quantum search [18–22]. For this model, the space of states $\mathcal{H}$ can be identified with the space spanned by the $M = 2^N$ spin states indicated by $|\boldsymbol{n}\rangle = |n_1\rangle|n_2\rangle \cdots |n_N\rangle$, where $|n_i\rangle = |\pm\rangle$ is an eigenstate of the Pauli matrix σ_i^z relative to qubit $i = 1, \ldots, N$. The potential is $V = \sum_{\boldsymbol{n}} V_{\boldsymbol{n}} |\boldsymbol{n}\rangle\langle\boldsymbol{n}|$, where $V_{\boldsymbol{n}} = -JN\delta_{\boldsymbol{n},\boldsymbol{n}_1}$, $J > 0$, and $\boldsymbol{n}_1$ represents the target of a totally unstructured (worst-case scenario) search. In contrast, structured searches correspond to potentials with a smooth minimum around the target and therefore benefit from the application of gradient-descent-based methods like the Ising model, in which, however, the corresponding QPTs are second order. Finally, the hopping operator K of the Grover model is chosen to be the sum of single-flip operators $K = -\sum_{i=1}^{N} \sigma_i^x$.

The GS of K is nondegenerate, and we choose $M_{\text{cond}} = 1$. It follows that $-\beta F_{\text{cond}} = -\beta V_1 = \beta JN$. Up to corrections exponentially small in N, the free energy of the normal subspace coincides with that of the hopping operator K, whose levels are $-\Gamma(N - 2j)$, $j = 0, \ldots, N$, and have degeneracy $N!/[j!(N-j)!]$,

$$e^{-\beta F_{\text{norm}}} = \text{tr}\, e^{-\beta K} = \sum_{j=0}^{N} \binom{N}{j} e^{-\beta[-\Gamma(N-2j)]}, \qquad (5)$$

which yields $-\beta F_{\text{norm}} = N \ln[2\cosh(\beta\Gamma)]$. The critical line defined by Eq. (3) is thus

$$J = k_B T \ln[2\cosh(\Gamma/k_B T)], \qquad (6)$$

which was also found in Ref. [22] via perturbation theory. Note that Eq. (6) has a solution only for $J \geqslant \Gamma$. A parametric plot of the critical line is shown in the inset of Fig. 2. For any fixed Γ, at high temperature Eq. (6) provides the asymptotic slope $T = J/(k_B \ln 2)$, while at low temperature the slope becomes infinite, in agreement with the quantum critical point $J = \Gamma$ of the $T = 0$ transition.

V. FREE FERMIONS IN A 1D INHOMOGENEOUS LATTICE

Finite-temperature condensation QPTs can be observed in a variety of physically relevant systems. Here, we study the case of N_p spinless fermions in a 1D lattice with $N \geqslant N_p$ sites. Some sites, the first consecutive $N_i < N_p$, for simplicity, differ from the others by the presence of an attractive potential so that the Hamiltonian of the system is

$$H = -\eta \sum_{l=1}^{N-1} (c_l^\dagger c_{l+1} + c_{l+1}^\dagger c_l) - g \sum_{l=1}^{N_i} c_l^\dagger c_l, \qquad (7)$$

where c_l is the fermionic annihilation operator on site l and we choose open boundary conditions. The hopping parameter η and the attractive strength g are positive constants. Note that we are considering a system of noninteracting particles; nevertheless, H is the sum of two noncommuting operators as in Eq. (1), and we can look for a condensation QPT by varying the parameter g.

First, we define the subspace $\mathcal{H}_{\text{cond}}$. Besides satisfying the necessary condition $M_{\text{cond}}/M \to 0$ in the TDL, this subspace

should be large enough for the free energies restricted to $\mathcal{H}_{\text{cond}}$ and $\mathcal{H}_{\text{norm}}$ to cross each other at some finite value g_c of the parameter g. The latter condition is equivalent to having $F_{\text{norm}}(g = 0) < F_{\text{cond}}(g = 0)$ and $\lim_{g \to \infty} F_{\text{cond}}(g)/g < \lim_{g \to \infty} F_{\text{norm}}(g)/g$; see Appendix C 1 for an analysis of this system in the $T = 0$ limit. In the present system and for $N_i = N_p$, the two inequalities above are satisfied if $M_{\text{cond}} = 1 + N_p^2$, i.e., if the subspace $\mathcal{H}_{\text{cond}}$ consists of the GS of V, in which all N_p fermions are in the N_i attractive sites, and also consists of the N_p^2 first excited states of V, in which $N_p - 1$ fermions are in the N_i attractive sites and one is in the remaining $N - N_i$ sites. Other choices of M_{cond} are possible, but they all lead to the same TDL. Remarkably, in this system, the nature of $\mathcal{H}_{\text{cond}}$ shows that a condensation in the space of states corresponds to an actual space localization in the attractive sites.

Second, we evaluate the order parameter (4) as

$$p_{\text{cond}} = \frac{1}{\sum_{j=1}^{M} e^{-\beta E_j}} \sum_{j=1}^{M} e^{-\beta E_j} \sum_{k=1}^{M_{\text{cond}}} |\langle \boldsymbol{n}_k | E_j \rangle|^2, \qquad (8)$$

where E_j and $|E_j\rangle$ are the N_p-particle eigenvalues and eigenvectors of H. These are easily obtained with Pauli's principle combining the single-particle eigenvalues and eigenvectors of H calculated by numerically diagonalizing the $N \times N$ tridiagonal matrix, whose nonzero elements are $A_{l+1,l} = A_{l,l+1} = -\eta$ for $l = 1, \ldots, N - 1$ and $A_{l,l} = -g$ for $l = 1, \ldots, N_i$. The computation of E_j and $|E_j\rangle$ is a simple task which requires a time $O(N^2)$. Also the computation of the sum of the squared scalar products in Eq. (8) requires an affordable time $O(N^2 N_p^2)$. In fact, the evaluation of the scalar product between the antisymmetrized states $|\boldsymbol{n}_k\rangle$ and $|E_j\rangle$ can be reduced to the evaluation of the determinant of the $N \times N$ matrix, whose elements are the projections of the single-particle eigenvectors of H in the basis of the eigenvectors of V [23]. The calculation of this determinant requires a time $O(N^2)$. It is the sum over M which limits the computation of p_{cond} to a relatively small number of particles; in fact, M grows as $N!/[N_p!(N - N_p)!]$.

In Fig. 1 we show the behavior of p_{cond} obtained as a function of the attractive strength g for a number of particles $N_p = 4, 6, 8, \ldots, 16$. As indicated above, we chose $N_p = N_i = N/2$ and $M_{\text{cond}} = 1 + N_p^2$. The equilibrium temperature is $k_B T/\eta = 0.2$; similar plots at different temperatures are provided in Appendix C 2. Whereas the order parameter exhibits a clear tendency toward the steplike behavior expected for a first-order QPT, we are still far from the TDL, and no classical supercomputer would allow us to reach much larger values of N_p. However, we can estimate the critical value g_c of the QPT, namely, the value of g at which $p_{\text{cond}} = 1/2$ in the TDL, using a fit-and-extrapolate procedure. The validity of this procedure in the case of the Grover model is illustrated in Appendix B. We fit the curve $a + b/N_p + c/N_p^2$ to the values of g at which $p_{\text{cond}} = 1/2$ for the available N_p and extrapolate $g_c = a$. A different fit model which provides a slowly diverging g_c, namely, $a + b \ln N_p + c \ln(\ln N_p)$, must be rejected as we obtain a pointless negative value of b (see the caption of Fig. 1).

In Fig. 2 we plot the values of g_c derived as explained above for different temperatures. The result is a phase diagram in the g-T plane having the same universal features [14] as the phase
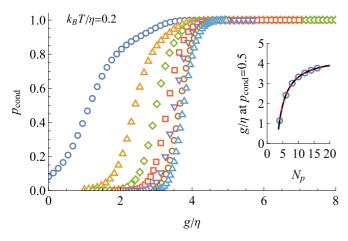
FIG. 1. Order parameter p_{cond} versus g/η for the fermionic system (7) with $N_p = N_i = N/2 = 4, 6, 8, 10, 12, 14, 16$, shown by symbols from left to right. Here, $M_{\text{cond}} = 1 + N_p^2$, and the system is at canonical equilibrium at temperature $k_B T/\eta = 0.2$. Inset: value of g/η at $p_{\text{cond}} = 1/2$ for different N_p. Data (circles) compare quite well ($\chi^2 \simeq 10^{-4}$) with two fitting models, $a + b/N_p + c/N_p^2$ (black solid line, $a = 4.424$, $b = 9.685$, and $c = 13.760$) and $a + b \ln N_p + c \ln(\ln N_p)$ (red dashed line, $a = 2.261$, $b = -2.268$, and $c = 7.627$). The second model, however, must be rejected because in the TDL it gives $g_c \to -\infty$.

diagram of the Grover model. This corroborates the existence of a condensation QPT for the present fermionic system.

The 1D fermionic system considered here can be investigated experimentally by using superlattices, grown with reliable technologies in the well-established two-dimensional semiconductor heterojunctions [24] or in 1D nanowires [25]. In both cases, the alternation of nanolayers of different materials forms effective 1D lattices made of wells and barriers obtained by the corresponding band gap energies. By varying the barrier widths and heights one can tune the hopping coefficients between neighboring wells, and by using
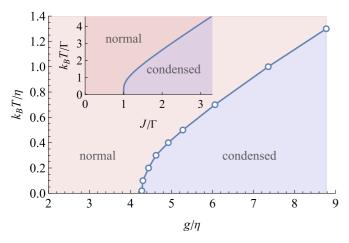

FIG. 2. Phase diagram g-T for the fermionic system (7). The solid line separating the two phases is obtained by connecting the dots evaluated by the fit-and-extrapolate procedure described in Fig. 1 for several values of $k_B T/\eta$. Inset: phase diagram J-T for the Grover model; the solid line separating the two phases is drawn according to Eq. (6).

different/doped materials one can adjust the bottom level of the wells, i.e., create local attractive potentials. The number of electrons in the nanocells of the superlattice can be fixed by photoexcitation, and their dislocation at thermal equilibrium can be detected by photoluminescence spectroscopy [26]. In this way, one can have direct access to the size-dependent order parameter and, for large superlattices in which the TDL has been effectively reached, to the critical line of the phase diagram.

VI. CONDENSATION QPTs AS EFFICIENT QUANTUM ANNEALERS

Quantum annealers [27] are physical devices generally aimed at exploiting the quantum adiabatic theorem [28] to solve several classes of optimization problems [29]: by gradually reducing Γ an initial disordered quantum state of the system, e.g., the GS of K in Eq. (1), is made to evolve toward the desired GS of V in a time τ roughly given by the inverse of the minimal gap of H. In fact, the adiabatic condition is usually formulated as $\tau = O(\Delta^{-2})$, with Δ being the minimal gap of H. However, for models in which the potential V is nondegenerate, the weaker condition $\tau = O(\Delta^{-1})$ turns out to be sufficient [20,30]. Therefore, the presence of a first-order QPT at Γ_c implies that τ may grow exponentially with N [20–22,30–32]. This is the case of the Grover model, in which the minimal gap is $2JN2^{-N/2}$, thus resulting in an adiabatic annealing protocol with the same complexity as Grover's algorithm [18,19]. This is in agreement with a general statement according to which, in terms of complexity, adiabatic and quantum gate-based protocols are equivalent [33].

In their basic definitions, both adiabatic annealing and quantum gate-based approaches require the system to be isolated and at $T = 0$. Of course, such ideal conditions are never satisfied, and although they are often tacitly assumed and/or supposed to be tackled by more and more robust and scalable technologies, they still represent a severe obstacle to the advance of real quantum computers. For annealers, the ideal $T = 0$ adiabatic protocol even remains ill defined when the time τ is not sufficiently long as excited states get populated, which implies heating, contrary to the initial assumption.

There have been attempts to extend adiabatic annealing to open systems at finite temperature. On the one hand, we have the result that open systems follow the instantaneous steady state of the associated Liouvillian provided that an adiabatic condition similar to that for isolated systems but with the gap of the Hamiltonian substituted by the gap of the Liouvillian [34–36] is satisfied. On the other hand, it is clear that out-of-equilibrium annealing offers a plethora of new possibilities, e.g., paths different from the adiabatic ones, which may provide advantages with respect to an adiabatic protocol [37–43]. Nevertheless, without a clear understanding of the thermodynamics of the quantum system, the whole picture remains incomplete.

Equations (2)–(4) reverse the fateful role of first-order QPTs, showing the following groundbreaking properties: (i) if a system admits a finite-temperature condensation QPT, it can work as a quantum annealer even if at finite temperature, i.e., not isolated. (ii) An annealing protocol consists of any path bringing the system from any point of the normal phase

to any point of the condensed phase. (iii) During the annealing protocol, the system does not need to stay at canonical equilibrium. (iv) If the system is at canonical equilibrium in the condensed phase, a measurement of its state will provide the target state with a probability (called output probability in [43]) exponentially close to 1 in size N [44].

Note that, in total contrast to statement (iv), in gate-based devices, the larger the size is, the larger the probability is that the device undergoes unwanted decoherence. Similarly, in quantum annealers operating away from a condensed phase, at $T > 0$ the output probability decreases exponentially with N [45]. It is in this sense that a quantum annealer based on a condensation QPT might offer a dramatically important advantage, exploiting, at best, the collective and spontaneous mechanism of phase transitions at finite temperature.

As an example application of statements (i)–(iv) above, consider the Grover model. It can work as an annealer due to its finite-temperature condensation. We can bring it from the normal to the condensed phase by following any path crossing the critical line given by Eq. (6) at some $T_c > 0$; in doing so, we are also free to follow out-of-equilibrium paths, provided we subtract from the system an amount of energy no smaller than the latent heat $L = N\{K_B T \ln[2\cosh(\beta\Gamma)] - \Gamma \tanh(\beta\Gamma)\}|_{T=T_c}$, easily derived from F_{cond} and F_{norm}. Once the model is in the condensed phase, a readout of the N spins of the model provides the target state with probability 1, up to corrections exponentially small in N.

Regrettably, the Grover Hamiltonian describes an abstract model. In fact, its potential V, which is totally unstructured, consists of the sum of two- to N-body interactions, a rather unphysical feature. On the other hand, the fermionic system in an inhomogeneous lattice could be implemented as a realistic quantum annealer. In the 1D lattice that we analyzed, however, the potential V is trivially structured, allowing for an efficient classical search of its GS (all fermions in the $N/2$ consecutive attractive sites). Nontrivial target states requiring an actual quantum search would be obtained by considering more general lattices, e.g., 1D lattices with attractive sites arranged in nontrivial ways and/or taking into account electron interaction. For all these systems a condensation QPT is still expected to manifest.

VII. CONCLUSIONS

We have extended to finite temperature a wide class of QPTs characterized by a condensation in the space of quantum states. Whereas a rigorous proof of these transitions was provided in [14] (see also Appendix A), here, we proposed an intuitive criterion based on the straightforward replacement of the ground-state energies with the corresponding free energies and checked the criterion in two different systems.

A main feature of this class of QPTs is that at any point of the condensed phase the canonical equilibrium state coincides with the system GS (one of the degenerate system GSs) with a probability exponentially close to 1 in the system size. We explained in detail how this feature may represent groundbreaking progress for quantum annealers; see statements (i)–(iv) expounded in the previous section.

Of course, understanding how long it takes for an annealer based on a condensation QPT to reach canonical equilibrium

in the condensed phase is crucially important but is out of the scope of the present paper. The thermalization of Grover's model or similar systems with a thermal bath represented by blackbody radiation could be tackled within the theories presented in [39,46]. It could be advantageous to consider annealers based on weakly short-range interacting systems for which rigorous bounds on the relaxation times exist in terms of those of the corresponding noninteracting systems [47]. We look forward to reporting the relative results.

APPENDIX A: PROOF OF EQUATIONS (2) AND (4)

For any partition $\mathcal{H} = \mathcal{H}_{\text{cond}} \oplus \mathcal{H}_{\text{norm}}$, we can prove (see Ref. [14]) that for any $|\boldsymbol{n}\rangle \in \mathcal{H}_X$ (X stands for either cond or norm and Y stands for its complement, norm or cond)

$$1 \leqslant \frac{\langle \boldsymbol{n}|e^{-\beta H}|\boldsymbol{n}\rangle}{\langle \boldsymbol{n}|e^{-\beta H_X}|\boldsymbol{n}\rangle} \leqslant e^{\beta\Gamma \min\{A_X^{(\text{out})}, A_Y^{(\text{out})}\}}, \quad (A1)$$

where $A_X^{(\text{out})} = \sup_{|\boldsymbol{n}\rangle \in \mathcal{H}_X} \sum_{|\boldsymbol{n}'\rangle \in \mathcal{H}_Y} |\langle \boldsymbol{n}|K|\boldsymbol{n}'\rangle|$ represents the maximum number of outgoing links (nonzero matrix elements of $K = H - V$) from $\mathcal{H}_X$ to $\mathcal{H}_Y$. The proof of Eq. (A1) is based on the exact probabilistic representation of the quantum evolution introduced in [13] used at an imaginary time which is identified with the inverse temperature β. The term $\min\{A_X^{(\text{out})}, A_Y^{(\text{out})}\}\Gamma$ represents the rate of convergence to 1 of the probability for crossing the boundary between $\mathcal{H}_X$ and $\mathcal{H}_Y$ as realized during an infinitely long evolution dictated by the Hamiltonian H. From Eq. (A1) we have (we here note that a harmless typo occurred in Eq. (18) of Ref. [14], where the term $-\ln(2)/\beta$ was missed on the right-hand side of that equation)

$$F \leqslant \min\{F_{\text{cond}}, F_{\text{norm}}\}, \quad (A2)$$

$$F \geqslant \min\{F_{\text{cond}}, F_{\text{norm}}\} - \min\{A_{\text{cond}}^{(\text{out})}, A_{\text{norm}}^{(\text{out})}\}\Gamma - \frac{\ln(2)}{\beta}. \quad (A3)$$

Equations (A2) and (A3) can be derived from (A1) as follows.

By using the left inequality of Eq. (A1) we have $\langle \boldsymbol{n}|e^{-\beta H}|\boldsymbol{n}\rangle \geqslant \langle \boldsymbol{n}|e^{-\beta H_X}|\boldsymbol{n}\rangle$, $\forall |\boldsymbol{n}\rangle \in \mathcal{H}_X$, and therefore,

$$\sum_{|\boldsymbol{n}\rangle \in \mathcal{H}} \langle \boldsymbol{n}|e^{-\beta H}|\boldsymbol{n}\rangle = \sum_{|\boldsymbol{n}\rangle \in \mathcal{H}_X} \langle \boldsymbol{n}|e^{-\beta H}|\boldsymbol{n}\rangle + \sum_{|\boldsymbol{n}\rangle \in \mathcal{H}_Y} \langle \boldsymbol{n}|e^{-\beta H}|\boldsymbol{n}\rangle$$

$$\geqslant \sum_{|\boldsymbol{n}\rangle \in \mathcal{H}_X} \langle \boldsymbol{n}|e^{-\beta H_X}|\boldsymbol{n}\rangle + \sum_{|\boldsymbol{n}\rangle \in \mathcal{H}_Y} \langle \boldsymbol{n}|e^{-\beta H_Y}|\boldsymbol{n}\rangle,$$

which means

$$e^{-\beta F} \geqslant e^{-\beta F_{\text{cond}}} + e^{-\beta F_{\text{norm}}} \geqslant e^{-\beta \min(F_{\text{cond}}, F_{\text{norm}})},$$

equivalent to Eq. (A2).

To prove Eq. (A3) we start from the right inequality of Eq. (A1), namely, $\langle \boldsymbol{n}|e^{-\beta H}|\boldsymbol{n}\rangle \leqslant \langle \boldsymbol{n}|e^{-\beta H_X}|\boldsymbol{n}\rangle e^{\beta \Gamma \min\{A_X^{(\mathrm{out})}, A_Y^{(\mathrm{out})}\}}$, $\forall |\boldsymbol{n}\rangle \in \mathcal{H}_X$, and obtain

$$
\sum_{|\boldsymbol{n}\rangle \in \mathcal{H}} \langle \boldsymbol{n}|e^{-\beta H}|\boldsymbol{n}\rangle
$$
$$
\leqslant \left(\sum_{|\boldsymbol{n}\rangle \in \mathcal{H}_X} \langle \boldsymbol{n}|e^{-\beta H_X}|\boldsymbol{n}\rangle + \sum_{|\boldsymbol{n}\rangle \in \mathcal{H}_Y} \langle \boldsymbol{n}|e^{-\beta H_Y}|\boldsymbol{n}\rangle \right)
$$
$$
\times e^{\beta \Gamma \min\{A_X^{(\mathrm{out})}, A_Y^{(\mathrm{out})}\}},
$$

which means

$$
e^{-\beta F} \leqslant \left(e^{-\beta F_{\mathrm{cond}}} + e^{-\beta F_{\mathrm{norm}}} \right) e^{\beta \Gamma \min\{A_{\mathrm{cond}}^{(\mathrm{out})}, A_{\mathrm{norm}}^{(\mathrm{out})}\}}
$$
$$
\leqslant 2 e^{-\beta \min(F_{\mathrm{cond}}, F_{\mathrm{norm}})} e^{\beta \Gamma \min\{A_{\mathrm{cond}}^{(\mathrm{out})}, A_{\mathrm{norm}}^{(\mathrm{out})}\}},
$$

equivalent to Eq. (A3).

Combining Eqs. (A2) and (A3) with the assumptions that F_{cond} and F_{norm} are extensive in N and that $\min\{A_{\mathrm{cond}}^{(\mathrm{out})}, A_{\mathrm{norm}}^{(\mathrm{out})}\} = o(N)$ proves that Eqs. (2) hold true up to terms becoming negligible in the TDL. In our setting, according to the definition of the subspace $\mathcal{H}_{\mathrm{cond}}$, we always have $\min\{A_{\mathrm{cond}}^{(\mathrm{out})}, A_{\mathrm{norm}}^{(\mathrm{out})}\} = A_{\mathrm{norm}}^{(\mathrm{out})} = o(N)$. This represents a reasonably general property. In the Grover model, for instance, we have $A_{\mathrm{norm}}^{(\mathrm{out})} = 1$, while $A_{\mathrm{cond}}^{(\mathrm{out})} = N$. Similarly, it is easy to check that in the model of free fermions in an inhomogeneous lattice, with the choice $N_p = N_i = N/2$ we have $A_{\mathrm{norm}}^{(\mathrm{out})} = 2$, while $A_{\mathrm{cond}}^{(\mathrm{out})} = N/2$. The important point is that, in most of the systems of interest, the conditions $M_{\mathrm{cond}}/M \to 0$ and $A_{\mathrm{norm}}^{(\mathrm{out})}/N \to 0$ are equivalent [14] and, under any of these conditions, Eqs. (A2) and (A3), up to $o(N)$ terms, provide Eqs. (2), namely, the generalization to finite temperature of the condensation QPTs, as suggested by the natural criterion of substituting GS energies with free energies.

To prove Eq. (4), we start inserting the expression of the Gibbs state $\rho = e^{-\beta H} / \operatorname{tr} e^{-\beta H}$ into the definition of p_{cond},

$$
p_{\mathrm{cond}} = \sum_{|\boldsymbol{n}\rangle \in \mathcal{H}_{\mathrm{cond}}} \langle \boldsymbol{n}|\rho|\boldsymbol{n}\rangle
$$
$$
= \frac{\sum_{|\boldsymbol{n}\rangle \in \mathcal{H}_{\mathrm{cond}}} \langle \boldsymbol{n}|e^{-\beta H}|\boldsymbol{n}\rangle}{\sum_{|\boldsymbol{n}\rangle \in \mathcal{H}} \langle \boldsymbol{n}|e^{-\beta H}|\boldsymbol{n}\rangle}
$$
$$
= \frac{1}{1 + \frac{\sum_{|\boldsymbol{n}\rangle \in \mathcal{H}_{\mathrm{norm}}} \langle \boldsymbol{n}|e^{-\beta H}|\boldsymbol{n}\rangle}{\sum_{|\boldsymbol{n}\rangle \in \mathcal{H}_{\mathrm{cond}}} \langle \boldsymbol{n}|e^{-\beta H}|\boldsymbol{n}\rangle}}. \tag{A4}
$$

By using again the left and right inequalities of Eq. (A1), we have the following inequalities, assuming $\min\{A_{\mathrm{cond}}^{(\mathrm{out})}, A_{\mathrm{norm}}^{(\mathrm{out})}\} = A_{\mathrm{norm}}^{(\mathrm{out})}$:

$$
p_{\mathrm{cond}} \leqslant \frac{1}{1 + \frac{\sum_{|\boldsymbol{n}\rangle \in \mathcal{H}_{\mathrm{norm}}} \langle \boldsymbol{n}|e^{-\beta H_{\mathrm{norm}}}|\boldsymbol{n}\rangle}{\sum_{|\boldsymbol{n}\rangle \in \mathcal{H}_{\mathrm{cond}}} \langle \boldsymbol{n}|e^{-\beta H}|\boldsymbol{n}\rangle}}
$$
$$
\leqslant \frac{1}{1 + \frac{\sum_{|\boldsymbol{n}\rangle \in \mathcal{H}_{\mathrm{norm}}} \langle \boldsymbol{n}|e^{-\beta H_{\mathrm{norm}}}|\boldsymbol{n}\rangle}{\sum_{|\boldsymbol{n}\rangle \in \mathcal{H}_{\mathrm{cond}}} e^{\beta \Gamma A_{\mathrm{norm}}^{(\mathrm{out})}} \langle \boldsymbol{n}|e^{-\beta H_{\mathrm{cond}}}|\boldsymbol{n}\rangle}} \tag{A5}
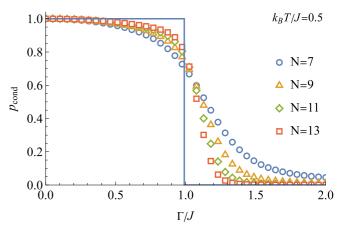$$

and

$$
p_{\mathrm{cond}} \geqslant \frac{1}{1 + \frac{\sum_{|\boldsymbol{n}\rangle \in \mathcal{H}_{\mathrm{norm}}} e^{\beta \Gamma A_{\mathrm{norm}}^{(\mathrm{out})}} \langle \boldsymbol{n}|e^{-\beta H_{\mathrm{norm}}}|\boldsymbol{n}\rangle}{\sum_{|\boldsymbol{n}\rangle \in \mathcal{H}_{\mathrm{cond}}} \langle \boldsymbol{n}|e^{-\beta H}|\boldsymbol{n}\rangle}}
$$
$$
\geqslant \frac{1}{1 + \frac{\sum_{|\boldsymbol{n}\rangle \in \mathcal{H}_{\mathrm{norm}}} e^{\beta \Gamma A_{\mathrm{norm}}^{(\mathrm{out})}} \langle \boldsymbol{n}|e^{-\beta H_{\mathrm{norm}}}|\boldsymbol{n}\rangle}{\sum_{|\boldsymbol{n}\rangle \in \mathcal{H}_{\mathrm{cond}}} \langle \boldsymbol{n}|e^{-\beta H_{\mathrm{cond}}}|\boldsymbol{n}\rangle}}. \tag{A6}
$$

On making use of the definitions of F_{cond} and F_{norm}, the two inequalities above can be rewritten as

$$
p_{\mathrm{cond}} \leqslant \frac{1}{1 + e^{-\beta(F_{\mathrm{norm}} - F_{\mathrm{cond}}) - \beta \Gamma A_{\mathrm{norm}}^{(\mathrm{out})}}},
$$
$$
p_{\mathrm{cond}} \geqslant \frac{1}{1 + e^{-\beta(F_{\mathrm{norm}} - F_{\mathrm{cond}}) + \beta \Gamma A_{\mathrm{norm}}^{(\mathrm{out})}}},
$$

which, on assuming again that $A_{\mathrm{norm}}^{(\mathrm{out})} = o(N)$, implies Eq. (4).
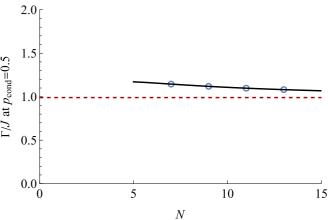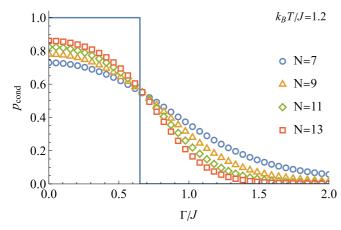

FIG. 3. Top: Order parameter p_{cond} versus Γ/J for the Grover model at thermal equilibrium at temperature $k_B T/J = 0.5$ for $N = 7, 9, 11, 13$ (open symbols). The steplike solid line is the asymptotic $N \to \infty$ exact value. Bottom: Value of Γ/J at $p_{\mathrm{cond}} = 1/2$ for different N (open circles). The function $a + b/N + c/N^2$ fits quite well the data (black solid line, $a = 0.96$, $b = 1.88$, and $c = -4.18$) and predicts the asymptotic exact value $\Gamma_c/J = 0.99$ (dashed red line) with a 3% error.
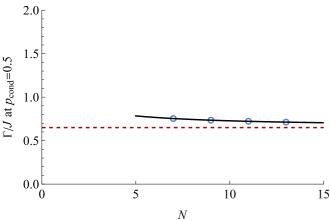
FIG. 5. Ground-state energy per particle E/N_p (blue line, right scale) and its first derivative with respect to the parameter g (red line, left scale) as a function of g/η for the system of free fermions in a 1D inhomogeneous lattice described by the Hamiltonian (7) with $N_p = N_i = N/2 = 133$. For this value of N_p both curves have practically reached their TDL.

FIG. 4. As in Fig. 3, but at temperature $k_B T/J = 1.2$. The fit parameters ($a = 0.67$, $b = 0.79$, and $c = -0.75$) predict the asymptotic exact value $\Gamma_c/J = 0.65$ with a 3% error.

APPENDIX B: ORDER PARAMETER OF GROVER MODEL

Figures 3 and 4 show the order parameter p_{cond} evaluated numerically in the Grover model as a function of Γ/J for different values of N. Note that the higher the temperature is, the slower the convergence of the data to the $N \to \infty$ limit of p_{cond} is, represented by the steplike solid line. Nevertheless, the fit of $a + b/N + c/N^2$ to the values of Γ/J at $p_{\text{cond}} = 0.5$ provides an asymptotic value of $\Gamma_c/J = a$ in good agreement with the exact value.

APPENDIX C: FREE FERMIONS IN A 1D INHOMOGENEOUS LATTICE

1. $T = 0$

First of all, we report the exact numerical analysis of the energy density E/N_p and its derivative $d(E/N_p)/dg$, as well as of the order parameter p_{cond} at $T = 0$. The zero-temperature case is particularly simple; we do not need to evaluate awkward canonical partition functions as in the case with $T > 0$, and we can consider systems of large size, with behavior practically indistinguishable from their TDLs.

Figure 5 clearly shows the presence of a point of nonanalyticity at $g_c = 4$ in the energy density of the system. This proves the existence of a QPT.
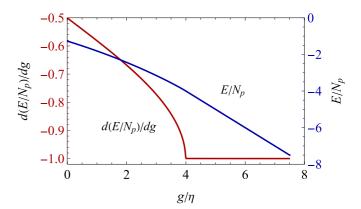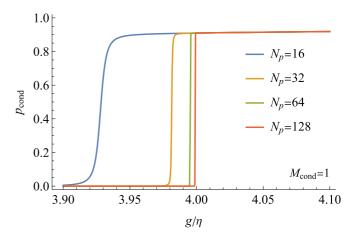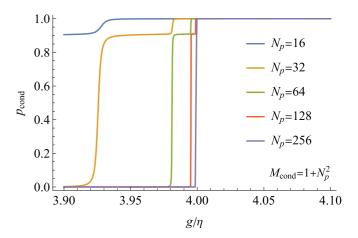

FIG. 6. Order parameter p_{cond} versus g/η at $T = 0$ for the system of free fermions in a 1D inhomogeneous lattice described by the Hamiltonian (7) with $N_p = N_i = N/2 = 16, 32, 64, 128, 256$. The top panel corresponds to the choice $M_{\text{cond}} = 1$, while in the bottom panel we have $M_{\text{cond}} = 1 + N_p^2$. In both panels p_{cond} has practically reached its TDL for the largest N_p shown.
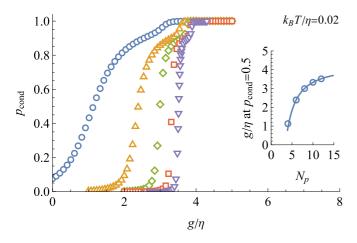
FIG. 7. Order parameter p_{cond} versus g/η for the fermionic system (7) with $N_p = N_i = N/2 = 4, 6, 8, 10, 12$ (symbols from left to right). We put $M_{\text{cond}} = 1 + N_p^2$, and the system is at canonical equilibrium at temperature $k_B T/\eta = 0.02$. Inset: value of g/η at $p_{\text{cond}} = 1/2$ for different N_p. Data (circles) compare quite well with the fitting function $a + b/N_p + c/N_p^2$ (solid line, $a = 4.277$, $b = -6.860$, and $c = -26.841$).
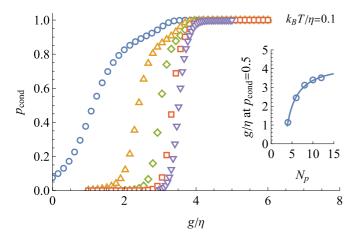

FIG. 8. As in Fig. 7, but at temperature $k_B T/\eta = 0.1$. The fit gives $a = 4.303$, $b = -7.058$, and $c = -22.568$.
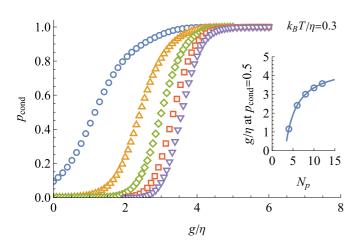

FIG. 9. As in Fig. 7, but at temperature $k_B T/\eta = 0.3$. The fit gives $a = 4.622$, $b = -11.987$, and $c = -7.506$.
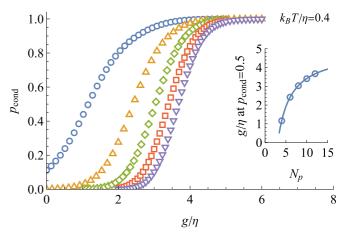

FIG. 10. As in Fig. 7, but at temperature $k_B T/\eta = 0.4$. The fit gives $a = 4.922$, $b = -15.144$, and $c = 0.4423$.
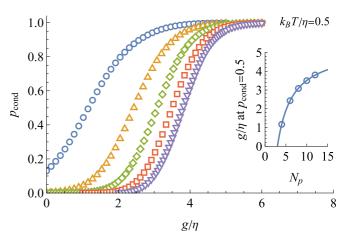

FIG. 11. As in Fig. 7, but at temperature $k_B T/\eta = 0.5$. The fit gives $a = 5.277$, $b = -18.517$, and $c = 8.364$.
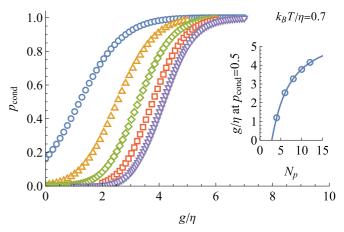

FIG. 12. As in Fig. 7, but at temperature $k_B T/\eta = 0.7$. The fit gives $a = 6.060$, $b = -24.931$, and $c = 21.991$.
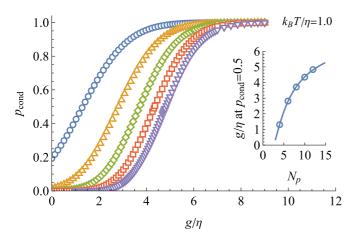
FIG. 13. As in Fig. 7, but at temperature $k_B T/\eta = 1.0$. The fit gives $a = 7.359$, $b = -33815$, and $c = 38.458$.

FIG. 14. As in Fig. 7, but at temperature $k_B T/\eta = 1.3$. The fit gives $a = 8.774$, $b = -42.407$, and $c = 52.764$.

Of course, the above result holds regardless of the choice of M_{cond}. In fact, in our approach any suitable choice of M_{cond}, e.g., $M_{\text{cond}} = 1$ or $M_{\text{cond}} = 1 + N_p^2$, will lead to the same critical point g_c. However, as shown in Fig. 6, only in the latter case do we have a complete jump of the order parameter p_{cond} between 0 and 1 at $g_c = 4$. According to Eq. (4), a 0–1 jump of p_{cond} at $g = g_c$ corresponds, for $T \to 0$, to a true crossing of the GS energies E_{cond} and E_{norm} at $g = g_c$ (more correctly, a true crossing of the TDL of the GS energy densities E_{cond}/N_p and E_{norm}/N_p). On the other hand, for $M_{\text{cond}} = 1$ the two energies E_{cond} and E_{norm}, which are distinct for $g < g_c$ (because $p_{\text{cond}} = 0$ and therefore $E_{\text{norm}} < E_{\text{cond}}$), merge and remain identical for $g \geqslant g_c$ (because $0 < p_{\text{cond}} < 1$). Note that for $M_{\text{cond}} = 1$ the order parameter slowly increases for $g > g_c$ and approaches 1 for $g \to \infty$. In this limit the GS $|E\rangle$ coincides with the lowest eigenstate of V, i.e., $|E\rangle \in \mathcal{H}_{\text{cond}}$. On the other hand, for any finite value $g \geqslant g_c$, $|E\rangle$ has components in both $\mathcal{H}_{\text{cond}}$ and $\mathcal{H}_{\text{norm}}$, with a net prevalence in the former. More precisely, the probability for the system to be found in $\mathcal{H}_{\text{cond}}$
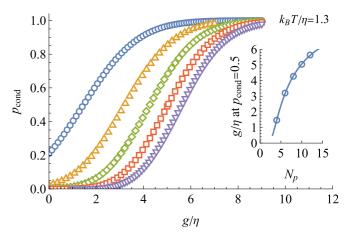
(i.e., in the lowest eigenstate of V) turns out to be larger than about 90% for $g \gtrsim g_c$.

It is interesting to observe the following technical aspect of the present QPT. From Fig. 5 we see that it is the second derivative of the energy density that diverges at $g = g_c$, whereas from Fig. 6 we see that the order parameter undergoes a finite jump at $g = g_c$. In other words, in this peculiar model, the QPT turns out to be a hybrid one which has a second-order nature (more precisely, it is a second-order transition within the so-called λ-transition class; see, for example, Ref. [6]) when seen with respect to the GS energy but a first-order nature when seen with respect to the order parameter.

2. $T > 0$

In Figs. 7–14, we report the values of p_{cond} obtained numerically for the system (7) at canonical equilibrium at different temperatures T. In each plot, the parameter a of the fit is taken as the critical value $g_c(T)$ shown in Fig. 2.

[1] S. L. Sondhi, S. M. Girvin, J. P. Carini, and D. Shahar, Continuous quantum phase transitions, Rev. Mod. Phys. **69**, 315 (1997).

[2] T. R. Kirkpatrick and D. Belitz, Quantum phase transitions in electronic systems, in *Electron Correlations in the Solid State*, edited by N. H. March (Imperial College Press, London, 1999), pp. 297–370.

[3] T. Vojta, Quantum phase transitions in electronic systems, Ann. Phys. (NY) **512**, 403 (2000).

[4] S. Sachdev, *Quantum Phase Transitions* (Cambridge University Press, Cambridge, 2000).

[5] P. Zanardi, H. T. Quan, X. Wang, and C. P. Sun, Mixed-state fidelity and quantum criticality at finite temperature, Phys. Rev. A **75**, 032109 (2007).

[6] H. T. Quan and F. M. Cucchietti, Quantum fidelity and thermal phase transitions, Phys. Rev. E **79**, 031101 (2009).

[7] L. D. Carr, *Understanding Quantum Phase Transitions* (CRC Press, Boca Raton, FL, 2010).

[8] A. Plastino and E. M. F. Curado, Finite temperature approach to quantum phase transitions, Int. J. Bifurcation Chaos **20**, 397 (2010).

[9] A. B. Finnila, M. A. Gomez, C. Sebenik, and D. J. Doll, Quantum annealing: A new method for minimizing multidimensional functions, Chem. Phys. Lett. **219**, 343 (1994).

[10] T. Kadowaki and H. Nishimori, Quantum annealing in the transverse Ising model, Phys. Rev. E **58**, 5355 (1998).

[11] G. E. Santoro and E. Tosatti, Optimization using quantum mechanics: Quantum annealing through adiabatic evolution, J. Phys. A **39**, R393 (2006).

[12] M. Ostilli and C. Presilla, First-order quantum phase transitions as condensations in the space of states, J. Phys. A **54**, 055005 (2021).

[13] M. Beccaria, C. Presilla, G. F. De Angelis, and G. Jona-Lasinio, An exact representation of the fermion dynamics in terms of Poisson processes and its connection with Monte Carlo algorithms, Europhys. Lett. **48**, 243 (1999).

[14] M. Ostilli and C. Presilla, Finite temperature quantum condensations in the space of states: General proof, J. Phys. A **55**, 505004 (2022).

[15] M. A. Continentino and A. S. Ferreira, First-order quantum phase transitions, J. Magn. Magn. Mater. **310**, 828 (2007).

[16] M. Campostrini, J. Nespolo, A. Pelissetto, and E. Vicari, Finite-Size Scaling at First-Order Quantum Transitions, Phys. Rev. Lett. **113**, 070402 (2014).

[17] M. Ostilli and C. Presilla, Wigner Crystallization of Electrons in a One-Dimensional Lattice: A Condensation in the Space of States, Phys. Rev. Lett. **127**, 040601 (2021).

[18] L. K. Grover, A fast quantum-mechanical search algorithm for database search, in *Proceedings of the Twenty-Eighth Annual ACM Symposium on the Theory of Computing* (ACM Press, New York, Philadelphia, Pennsylvania, 1996), pp. 212–219; Quantum Mechanics Helps in Searching for a Needle in a Haystack, Phys. Rev. Lett. **79**, 325 (1997); From Schrödinger's equation to the quantum search algorithm, Am. J. Phys. **69**, 769 (2001).

[19] J. Roland and N. J. Cerf, Quantum search by local adiabatic evolution, Phys. Rev. A **65**, 042308 (2002).

[20] E. Farhi, J. Goldstone, S. Gutmann, and D. Nagaj, How to make the quantum adiabatic algorithm fail, Int. J. Quantum Inf. **06**, 503 (2008).

[21] T. Jörg, F. Krzakala, J. Kurchan, and A. C. Maggs, Simple Glass Models and Their Quantum Annealing, Phys. Rev. Lett. **101**, 147204 (2008).

[22] T. Jörg, F. Krzakala, J. Kurchan, A. C. Maggs, and J. Pujos, Energy gaps in quantum first-order mean-field–like transitions: The problems that quantum annealing cannot solve, Europhys. Lett. **89**, 40004 (2010).

[23] J. P. Blaizot and G. Ripka, *Quantum Theory of Finite Systems* (MIT Press, Cambridge, MA, 1986).

[24] Q. Wang, L. Zhang, X. Liu, and S. Li, Two-dimensional semiconductor heterojunctions for optoelectronics and electronics, Front. Energy Res. **9**, 802055 (2021).

[25] O. Arif, V. Zannier, F. Rossi, D. De Matteis, K. Kress, M. De Luca, I. Zardo, and L. Sorba, GaAs/GaP superlattice nanowires: Growth, vibrational and optical properties, Nanoscale **15**, 1145 (2023).

[26] D. Tedeschi, M. De Luca, and A. Polimeni, Photoluminescence spectroscopy applied to semiconducting nanowires: A valuable probe for assessing lattice defects, crystal structures, and carriers' temperature, in *Fundamental Properties of Semiconductor Nanowires*, edited by N. Fukata and R. Riccardo (Springer, Singapore, 2021), pp. 289–306.

[27] T. Lanting, A.J. Przybysz, A.Yu. Smirnov, F.M. Spedalieri, M.H. Amin, A.J. Berkley, R. Harris, F. Altomare, S. Boixo, P. Bunyk *et al.*, Entanglement in a Quantum Annealing Processor, Phys. Rev. X **4**, 021041 (2014).

[28] T. Kato, On the adiabatic theorem of quantum mechanics, J. Phys. Soc. Jpn. **5**, 435 (1950).

[29] E. Farhi and S. Gutmann, Analog analogue of a digital quantum computation, Phys. Rev. A **57**, 2403 (1998).

[30] J. Adame and S. Warzel, Exponential vanishing of the ground-state gap of the quantum random energy model via adiabatic quantum computing, J. Math. Phys. **56**, 113301 (2015).

[31] B. Altshuler, H. Krovi, and J. Roland, Anderson localization makes adiabatic quantum optimization fail, Proc. Natl. Acad. Sci. USA **107**, 12446 (2010).

[32] C. Presilla and M. Ostilli, Phase transitions and gaps in quantum random energy models, Physica A (Amsterdam, Neth.) **515**, 57 (2019).

[33] D. Aharonov, W. van Dam, J. Kempe, Z. Landau, S. Lloyd, and O. Regev, Adiabatic quantum computation is equivalent to standard quantum computation, SIAM Rev. **50**, 755 (2008).

[34] J. E. Avron, M. Fraas, G. M. Graf, and P. Grech, Adiabatic theorems for generators of contracting evolutions, Commun. Math. Phys. **314**, 163 (2012).

[35] L. Campos Venuti, T. Albash, D. A. Lidar, and P. Zanardi, Adiabaticity in open quantum systems, Phys. Rev. A **93**, 032118 (2016).

[36] A. Joye, Adiabatic Lindbladian evolution with small dissipators, Commun. Math. Phys. **391**, 223 (2022).

[37] M. S. Sarandy and D. A. Lidar, Adiabatic approximation in open quantum systems, Phys. Rev. A **71**, 012331 (2005).

[38] M. H. S. Amin, P. J. Love, and C. J. S. Truncik, Thermally Assisted Adiabatic Quantum Computation, Phys. Rev. Lett. **100**, 060503 (2008).

[39] L. Campos Venuti, T. Albash, M. Marvian, D. Lidar, and P. Zanardi, Relaxation versus adiabatic quantum steady-state preparation, Phys. Rev. A **95**, 042302 (2017).

[40] A. Mishra, T. Albash, and D. A. Lidar, Finite temperature quantum annealing solving exponentially small gap problem with non-monotonic success probability, Nat. Commun. **9**, 2917 (2018).

[41] G. Passarelli, G. De Filippis, V. Cataudella, and P. Lucignano, Dissipative environment may improve the quantum annealing performances of the ferromagnetic *p*-spin model, Phys. Rev. A **97**, 022319 (2018).

[42] G. Passarelli, V. Cataudella, and P. Lucignano, Improving quantum annealing of the ferromagnetic *p*-spin model through pausing, Phys. Rev. B **100**, 024302 (2019).

[43] E. J. Crosson and D. A. Lidar, Prospects for quantum enhancement with diabatic quantum annealing, Nat. Rev. Phys. **3**, 466 (2021).

[44] For simplicity, we assumed that the potential *V* has a nondegenerate GS, as in the Grover model or the fermionic system. If the GS of V has degeneracy *d*, statement (iv) needs to be rephrased as follows: if the annealer is at canonical equilibrium in the condensed phase, a measurement of its state will provide one of the *d* target states with a probability exponentially close to 1 in the size *N*.

[45] T. Albash, V. Martin-Mayor, and I. Hen, Temperature Scaling Law for Quantum Annealing Optimizers, Phys. Rev. Lett. **119**, 110502 (2017).

[46] M. Ostilli and C. Presilla, Thermalization of noninteracting quantum systems coupled to blackbody radiation: A Lindblad-based analysis, Phys. Rev. A **95**, 062112 (2017).

[47] L. Bertini, A. De Sole, G. Posta, and C. Presilla, Perturbative criteria for the ergodicity of interacting dissipative quantum systems (unpublished).